NASA Technical Memorandum 82846

Nonlinear Structural and Life Analyses of a Combustor Liner

(NASA-TM-82846) NONLINEAR STRUCTURAL AND LIFE ANALYSES OF A COMBUSTOR LINER (NASA) 23 p HC A02/MF A01 CSCL 20K

N82-24501

Unclas

G3/39 09902

V. Moreno and G. J. Meyers
United Technologies Corporation
Pratt and Whitney Aircraft Group
East Hartford, Connecticut

and

A. Kaufman and G. R. Halford
Lewis Research Center
Cleveland, Ohio

Prepared for the
Symposium on Advances and Trends in Structural and Solid Mechanics
cosponsored by NASA and Georgetown University
Washington, D.C., October 4-7, 1982

NASA

E-1216

NONLINEAR STRUCTURAL AND LIFE ANALYSES OF A COMBUSTOR LINER

V. Moreno and G. J. Meyers*

and

A. Kaufman and G. R. Halford†

ABSTRACT

Three dimensional, nonlinear finite-element structural analyses were performed for a simulated combustor liner specimen to assess the capability of nonlinear analyses using classical inelastic material models to represent the thermoplastic-creep response of the one-half scale component. The structural analysis results indicated continued cyclic hardening and ratchetting while experimental data suggested a stable stress-strain response after only a few loading cycles. In addition, the computed stress-strain history at the critical location was input into two life prediction methods, Strainrange Partitioning and a Pratt and Whitney Combustor Life Prediction Method, to evaluate their ability to predict cyclic crack initiation. The life prediction analyses overpredicted the observed cyclic crack initiation life.

*United Technologies Corporation, Pratt & Whitney Aircraft Group, East Hartford, Connecticut 06108.

†NASA Lewis Research Center, 21000 Brookpark Road, Cleveland, Ohio 44135.

INTRODUCTION

The overall operating cost of the modern gas turbine engine is significantly affected by the efficiency, performance level, emission goals, and durability associated with the major hot section components. These are the combustor and turbine structures in the engine. During each flight cycle, these components undergo large thermally induced stress-strain cycles which may include significant amounts of creep and relaxation that directly impact on durability. Assessment of durability requires detailed knowledge of the operating environment and the ability to accurately calculate structural response at the critical locations from which cracks initiate and propagate.

Nonlinear finite-element computer programs such as the MARC (1)* code are available for the 3-dimensional structural analysis of engine components subject to cyclic thermomechanical loading. These programs involve sophisticated computational algorithms and advanced finite element formulations, yet rely on material models whose applicability to the hot section component environment is questionable. Of primary concern is the response of materials to cyclic loading involving simultaneous creep and plastic behavior. A major need is the development of appropriate hot section component strain and life data, sufficient to evaluate the advanced structural analysis and life prediction methodologies.

This study addresses a critical issue in the development of advanced life prediction technologies - establishing the limitations of current nonlinear structural modeling and creep-fatigue life prediction schemes for a major hot section component. In order to make a critical evaluation of these tools, a

---

*Numbers in brackets designate References at end of paper.

well-controlled component simulation test served as the calibration data source for the program. The component test used a one half scale combustor liner specimen constructed in an identical configuration with current combustor liners in engine service.

A three dimensional nonlinear finite element analysis of the liner was conducted with the MARC computer code. The analysis used existing time-independent classical plasticity theory with a Von Mises yield surface and the combined (isotropic-kinematic) hardening rule. A constant rate creep model was used to account for instantaneous time-dependent inelasticity effects. Both the plasticity and creep models were calibrated to isothermal Hastelloy X material response data. Also, the computed strain-temperature history at the critical location of the combustor liner was imposed on a uniaxial specimen in a strain-temperature controlled test. The uniaxial results were compared to the analytical stress-strain results. The computed inelastic strain response was used as input into two life prediction methods [Strainrange Partitioning (2) and a Pratt and Whitney Combustor Life Prediction Method (3)] and the predicted combustor cyclic crack initiation life was compared against experimental observations.

PROBLEM DESCRIPTION

A combustor liner specimen of the conventional louver type of construction such as illustrated in Figure 1, was selected for evaluation in this program. The specimen was fabricated of Hastelloy X sheet for which temperature-dependent physical properties are presented in Table I. The combustor liner specimen was subjected to cyclic thermal loading in an induction heated experimental rig (4). Using known heat flux and cooling airflow rates as input, transient and steady-state, 3 dimensional heat transfer analyses were conducted. The computed temperature response (Figure 2) of the middle louver of the liner specimen closely agreed with measured thermocouple data. The

90-second test cycle consisted of a 20-second transient from an isothermal, 504°C minimum temperature to a 954°C maximum temperature, a 40-second steady-state portion, and a cool down back to the original isothermal condition. After the 20-second heating transient there was a temperature difference between the knuckle and louver lip of approximately 400°C. A total of 1730 cycles were accumulated on the test specimen. Cracking was observed at the edge of the louver lip after 1000 cycles of testing.

ANALYTICAL PROCEDURE

The MARC general purpose finite element program was used to predict the structural response of the louver to the thermal and mechanical loads. In evaluating the response the program assumes that the loading history is divided into a number of incrementally applied loading steps. Each load step is then sequentially analyzed as a linear problem using an appropriate stiffness matrix and load vector.

For the nonlinear analysis, each cycle was subdivided into a total of 78 steps consisting of 35 thermal load increments during heating, 14 creep increments during the steady-state hold times, 25 thermal load increments during cooling and an additional 4 no-load increments during the creep analysis for residual load correction, as discussed below, to ensure equilibrium.

The plasticity algorithm in MARC is based on a tangent stiffness approach, in which the stiffness matrix is updated and reassembled for every plastic loading increment. An iterative scheme is then used to calculate the response of the structure to each individual load increment. When the strain energy used to estimate the stiffness matrix in the assembly phase is approximately equal to the strain energy obtained in the solution phase, the iteration is terminated and the program proceeds to the next loading increment. If

convergence is not obtained within a specified number of cycles, the program will terminate with an appropriate error message. To ensure that the solution does not drift from a state of equilibrium as loading progresses, the applied incremental load vector, ΔP, is modified by the addition of a residual load correction vector, P-I. This vector is obtained by taking the sum of the internal reactions, I, and subtracting them from the total external load vector, P. The residual load vector from the (n-1)th increment is then used to augment the applied incremental load vector in the nth increment.

For general use in structures undergoing small deformation, the program uses the Prandtl-Reuss stress-strain equations of classical plasticity with a Von Mises yield surface. A combined isotropic-kinematic hardening option which allows the yield surface to expand and translate was considered as the appropriate model to represent the cyclic material response. A piecewise linear representation of the monotonic stress-strain curves was provided through a user subroutine.

The nonlinear algorithm employed in the program assumes that the total strain may be additively split into elastic, plastic, and creep components. The plastic strain, ϵ_{pl}, is determined during the plastic loading phase according to rate-independent plasticity theory. It is assumed that the prior creep strain, ϵ_{cr}, does not affect the subsequent plastic response, so that no interaction effects are included in the constitutive theory.

The creep option allows time-dependent effects to be included by assuming that the creep response equations are constitutive equations which are valid not only for constant stress histories, but for general stress histories. The program algorithm treats the nonlinearities due to the creep "constitutive relation" by incorporating them into a suitable load vector and modifying them by an initial strain technique. Thus, during small deformation creep, the

stiffness matrix remains constant and only the load vector is changed on an incremental basis. Since the stiffness matrix is constant, the reassembly of this matrix is avoided and the program solves for the incremental displacements by matrix back substitution. It has been demonstrated that this results in typical incremental computer times which are about 50 percent of the computer time required for the assembly and solution required in a plastic loading increment. An automatic time stepping scheme is incorporated into the solution algorithm to reduce computing time during the creep process.

MATERIAL MODELING

The Hastelloy X sheet material is highly strain rate sensitive at the temperatures of interest. The approach used for development of the Hastelloy X material plasticity model considered a tri-linear representation of the monotonic tensile curves and the cyclic hardening rule. These curves were determined from tests conducted at a strain rate 0.8 percent per min.. This strain rate is representative of the rates determined from a preliminary structural analysis of the specimen. Using this approach, the monotonic stress-strain curves for temperatures between 427°C and 982°C were constructed and incorporated into the user subroutine. The stress-strain representation used in the louver analysis is presented in Figure 3. Because of the cyclically stable behavior of this alloy, the monotonic stress-strain curves were justified for use in the cyclic stress-strain analysis.

A creep solution which was included in the analysis modeled the time dependent material response. This required that the incremental plasticity

solution be periodically stopped and creep allowed to occur. The material creep response was incorporated into another user subroutine in the form:

$$\varepsilon_{cr} = (\sigma/A)^n \, t,$$

where, ε_{cr} = creep strain

σ = stress

t = time

A, n = temperature-dependent constants

Simulation of the instantaneous time-dependent nature of the high temperature material response required that the constants be determined from short time (<1 minute), high stress level ($\sigma \geq 0.6\ \sigma_{yield}$) Hastelloy X creep data. The constants of the creep response equation are presented as a function of temperature in Table II.

FINITE ELEMENT MODELING

The three dimensional (3D) finite element model of the louver of the test specimen is shown in Figure 4. The model contains an included angle of slightly greater than 0.5° which represents the distance between the radial symmetry planes of two adjacent cooling holes. This small model size was selected because of the circumferentially uniform temperatures in the louver lip region and in an attempt to minimize computer run time.

As shown in Figure 4 the model consists of 30 elements. The majority of the elements are the 20 node isoparametric element with reduced integration using 8 Gaussion points. Since it is known that some reduced integration point elements are unreliable if distorted shapes are used (1), the full 27 integration point element was used around the cooling holes. The selection of the reduced integration point elements was based on initial estimates of the savings in run time over the full integration point element.

In the actual louver, the seam weld extends only over a portion of the overlapping sheets (Figure 1). During the heating portion of the test cycle

the hotter louver lip wants to expand radially a larger amount than the colder knuckle and cooling hole region. This results analytically in overlapping of the structure in this region which is an impossibility. Analyses conducted using the node tying option in MARC to prevent the overlapping of these nodes indicated a 13 percent increase in hoop mechanical strain relative to the case where overlapping was allowed to occur.

The philosophy used for the 3D model was to tie the nodes to prevent overlapping during the heating and steady state portions of the cycle and then untie the nodes during the cooling portion of the cycle.

The effect of the complete shell structure was simulated by appropriate boundary conditions. Along all initially radial edge planes only nodal displacements along these radial planes were permitted. Additional boundary conditions were imposed to simulate the restraint of the fore and aft louvers of the test specimen, these conditions required that nodal displacements on the front plane of the fore louver be related to nodal displacements on the rear plane of the aft louver by the ratio of the original radii of the fore and aft louver planes.

The 3D model used 640K double precision words of storage on an IBM 370/3033 computer system. Each analytical cycle required approximately 45 minutes of execution time.

DISCUSSION OF ANALYTICAL RESULTS

The fatigue critical location of the combustor liner specimen is the edge of the louver lip. The observed failure mode is axial cracking from the edge toward the weld. Results of the structural analysis indicated that this location experiences essentially a uniaxial, hoop stress field. In the following discussion, the predicted hoop stress/strain components at the element integration point closest to the edge have been used to define the response.

Initially, a linear elastic analysis was conducted to provide a baseline for comparison with the nonlinear results. The elastic analysis used the same finite element model and thermal loading increments as were input into the nonlinear analysis. Identical material properties were also used, but with two exceptions. Creep was not considered, and the yield points were set at arbitrarily high values to prevent yielding in the elastic case.

Figure 5 shows the computed elastic stress-strain response at the critical location. Letter designations are given on Figure 5 so the response can be followed using the same letter designations given for the temperature response in Figure 2. During the heating portion of the cycle the metal temperatures increased from 504°C at startup (A) to 954°C at the end of heating (D). The minimum mechanical strain occurred after 12.5 seconds of heating (C) when the temperature was 921°C. The maximum mechanical strain occurred 78 seconds into the cycle (F) or after 18 seconds of cooling when the temperature was 513°C.

Predicted results from the liner nonlinear analysis for the first two thermal loading cycles are shown in Figure 6 with letter designations similar to those shown for the temperature response (Figure 2). Initial yielding took place on the first cycle after 5 seconds heating (B) at a temperature of 732°C. Plastic flow occurred between B and C. Creep analyses were conducted between 12.5 seconds heating (C) and 60 seconds (D) when the heating portion of the cycle was completed. The reverse yield point was reached 66 seconds into the cycle or after 6 seconds of cooling (E). Subsequent loading for the second cycle produced reyielding at a temperature of 893°C (B') as compared to 732°C (B) for the first cycle. The other points indicated for the second cycle (C' to F') occurred at similar times and temperatures as in the first cycle.

As shown in Figure 7, the predicted stress-strain response at the edge of the louver lip had not stabilized after 6 thermal loading cycles. The mean strain and stress values were still changing and the amount of cyclic inelastic strain per cycle was decreasing. Cycles 2 to 6 show similar stress-strain loops which ratchet in the negative strain direction. Each succeeding cycle exhibited higher peak tensile stresses during cooling; however, the total strain range was essentially constant for all cycles.

Elastic and inelastic analysis results for the louver lip are compared in Table III. The cyclic hoop strain range predicted with the elastic analysis is within 8 percent of that predicted from the sixth cycle of the nonlinear analysis. Peak and mean stress-strain levels are considerably different between the analyses.

To provide material response data for further evaluation of the material models used in the nonlinear analysis of the combustor liner specimen, thermomechanical testing was conducted on a smooth, uniaxial specimen. The experimental system (5) is capable of following a prescribed strain-temperature history.

The predicted hoop mechanical strain and temperature histories for the sixth thermal loading cycle at the edge of the louver lip were used to define the specimen test conditions. Because the region near the edge of the louver lip experiences a uniaxial stress field, the stress-strain output from the specimen test is considered representative of the actual response producing the fatigue failure.

The thermomechanical strain cycling demonstrated that the stress-strain response stabilized during the first few cycles and no significant mean or peak stress changes occurred on subsequent cycling. Reverse plasticity was observed during the cooling portion of the cycles. Further investigation of

the ability of the material models to reproduce the experimental results were conducted with a one dimensional, strain-controlled analytical simulation of the experiment. This analysis used the same creep-plasticity models as the 3D louver analysis and was run through the same mechanical strain-temperature history as the specimen test. The simplicity of the analysis allowed a larger number of cycles to be economically run to evaluate material cyclic response.

The results of the stable uniaxial thermomechanical test and the nonlinear analyses for the 15th and 30th cycles are compared in Figure 8. The predicted stress-strain response did not stabilize and showed a larger mean stress and a smaller amount of cyclic inelastic strain than the test stress-strain loop. These discrepancies betweeen predicted and experimental cyclic response may be due to the uncoupling of the creep and plasticity models used in the analysis. Improving the accuracy of the predicted stress-strain response under cyclic thermomechanical loading may require use of one of the unified constitutive theories now undergoing development (see 6). These unified theories combine creep and plasticity effects by means of strain-rate dependent viscoplastic models. Determination of the correct thermomechanical response is critical for realistic life prediction of the component.

LIFE PREDICTION

The two high-temperature, creep-fatigue life prediction methods considered were the Strainrange Partitioning (SRP) and the Pratt and Whitney Aircraft - Commercial Products Division (PWA-CPD) Combustor Life Prediction Methods. Both assume that time-independent plastic and time-dependent creep damage mechanisms are present at elevated temperature. Isothermal creep-fatigue and creep rupture tests are used to define the material life relationship for these methods.

The SRP and PWA-CPD Methods are based on the existence of generic types of fully reversed damage cycles composed of combinations of the plastic and creep deformation mechanisms. For this analysis the combustor louver lip response contains only the pp(tensile plasticity reversed by compressive plasticity) and pc(tensile plasticity reversed by compressive creep) damage cycles. A more complete discussion of both life prediction methods and their application to the current problem are contained in (4).

All of the louver lip information presented heretofore was predicted at the integration point closest to the edge of the lip. For the crack initiation life predictions the strains were extrapolated to the corner of the louver lip by a quadratic extrapolation procedure.

The initial life prediction with the SRP method used the results from the 6th loading cycle of the nonlinear analysis. The pp and pc components were determined from the plastic strain change from B' to C' (Figure 6), the creep strain change from C' to D' (Figure 6), and the tensile plastic strain change from E' to F' (Figure 6). These values were $\Delta\varepsilon_{pp} = .025$ percent and $\Delta\varepsilon_{pc} = .06$ percent at the element integration point and $\Delta\varepsilon_{pp} = .0294$ percent and $\Delta\varepsilon_{pc} = .0705$ percent extrapolated to the corner of the louver lip. Hence, the inelastic strain range, $\Delta\varepsilon_{in} = 0.100$ percent with $F_{pp} = \Delta\varepsilon_{pp}/\Delta\varepsilon_{in} = 0.294$ and $F_{pc} = \Delta\varepsilon_{pc}/\Delta\varepsilon_{in} = 0.706$. The corresponding lives, $N_{pp} = 10600$ and $N_{pc} = 7850$ determined from the experimentally determined SRP life relations of Reference (4) lead to a predicted life, N_{pr}:

$$\frac{1}{N_{pr}} = \frac{F_{pp}}{N_{pp}} + \frac{F_{pc}}{N_{pc}} \quad ; \quad N_{pr} = 8500$$

The observed crack initiation life was within the range of 1000 to 1250 cycles.

The PWA-CPD Combustor Life Prediction Method is conceptually the same as the SRP Method. However, the inelastic strain components ($\Delta\epsilon_{pp}$ and $\Delta\epsilon_{pc}$) are determined from relationships based on the total mechanical strain range. The resulting quantities are $\Delta\epsilon_{pp}$ = .221 percent and $\Delta\epsilon_{pc}$ = .068 percent. These inelastic strains, particularly $\Delta\epsilon_{pp}$, are not only larger than those determined from the nonlinear analysis, but are also larger than the observed inelastic strain in the thermomechanical specimen. The PWA-CPD Method utilized PP and PC life relations that are derived from the Ductility-Normalized-SRP life relations as discussed in Reference (4). Furthermore, the linear, rather than the interaction damage rule is used. Hence, the predicted life N_{pr} is calculated from the following equation, with N_{pp} and N_{pc} life values of 3300 and 3600 respectively:

$$\frac{1}{N_{pr}} = \frac{1}{N_{pp}} + \frac{1}{N_{pc}} \quad ; \quad N_{pr} = 1700$$

which is in reasonably good agreement with the observed crack initiative life of 1000 to 1250 cycles. If the smaller inelastic strain range obtained from the nonlinear analysis was used, the PWA-CPD Method would predict 8000 cycles or about the same life as the SRP Method. It must be emphasized that in actual design practice, the PWA-CPD Method is used in conjunction with experimental and field sevice data to assess the overall service life of the component.

The crack initiation life prediction methods used isothermal, laboratory test data. The overpredictions in life resulting from the isothermal methods suggest that thermal cycling produces damage at a faster rate than comparable isothermal cycling. Research is being planned to study the differences between thermal and isothermal cycling.

SUMMARY OF RESULTS

The results of the combustor liner nonlinear structural and life analyses can be summarized as follows:

1. The nonlinear structural analysis indicated that the time-independent plasticity model and the time-dependent creep model did not accurately predict the cyclic thermomechanical response at the louver failure location. Tests of a uniaxial strain controlled specimen run with the same mechanical strain-temperature history as computed at the failure location showed that the stress-strain response stabilized within the first few cycles. Analytical simulation of this experiment with the Hastelloy X creep-plasticity models exhibited continued cyclic hardening (increasing peak tensile stress and reduced inelastic strainrange) and ratchetting after many cycles.

   Use of one of the rate-dependent (unified) constitutive theories currently under development may be required to improve the prediction for the varying temperature loading condition. Determination of correct thermomechanical response is critical for the life prediction of engine hot section components.

2. The linear elastic structural analysis and the nonlinear inelastic analysis predicted total strainrange values that were within 8 percent of one another. In addition, the inelastically calculated total strainrange remained constant even though the stresses and strains ratchetted.

3. The two high-temperature, creep-fatigue life prediction methods considered were the Strainrange Partitioning and the Pratt and Whitney Aircraft-Commercial Products Division Combustor Life Prediction Methods. Both methods are based on the existence of generic types of reversed inelastic strain cycles composed of combinations of the plastic and creep

mechanisms. For this analysis, the combustor louver lip response is composed of the pp(tensile plasticity reversed by compressive plasticity) and pc (tensile plasticity reversed by compressive creep) damage cycles. The Strainrange Partitioning Method overpredicted the louver cracking life (8500 cycles vs. 1000 cycles).

The Pratt and Whitney-Commercial Products Division Method also over-predicted the louver cracking life (1700 cycles vs. 1000 cycles). This improved correlation, relative to SRP, is due primarily to a larger pre-dicted inelastic strainrange. Using the smaller, more realistic inelastic strainrange computed from the nonlinear analysis resulted in a predicted life of 8000 cycles, which is similar to the SRP results. In actual design practice, the PWA-CPD method is used with experimental and field service data to assess the overall service life of the component.

4. The overpredictions in the combustor liner life based on the analyses in conjunction with isothermal, strain-controlled fatigue test data suggest that a thermomechanical fatigue cycle produces damage at a faster rate than a comparable isothermal cycle.

REFERENCES

1. "MARC General Purpose Finite Element Program, Users Manual", Volumes A-E, MARC Analysis Research Corporation, 1981.
2. "Characterization of Low Cycle High Temperature Fatigue by the Strain-range Partitioning Method", AGARD-CP-243, Technical Editing and Reproduction Ltd., London, 1978.
3. Schlein, B. C., "Reliability Prediction for Combustors and Turbines", AFAPL-TR-77-8, 1977.
4. Moreno, V., "Combustor Liner Durability Analysis", NASA CR-165250, 1981.

5. Hopkins, S. W., "Low Cycle Thermal Mechanical Fatigue Testing", Thermal Fatigue of Materials and Components, ASTM STP 612, American Society for Testing Materials, 1976, pp. 157-169.

6. Walker, K. P., "Research and Development Program for Nonlinear Structural Modeling with Advanced Time-Temperature Dependent Constitutive Relationships", NASA CR-165533, 1981.

ORIGINAL PAGE IS
OF POOR QUALITY

TABLE I. - TEMPERATURE-DEPENDENT PHYSICAL PROPERTIES USED IN LOUVER ANALYSIS

Temperature, °C	Proportional limit		Modulus of elasticity, 10^3 MPa	Mean coefficient of thermal expansion, 10^{-3} %/°C	Poisson's ratio
	Stress, MPa	Strain, percent			
505	316	0.186	170	1.49	0.326
538	316	.186	170	1.50	.328
649	304	.189	161	1.54	.334
760	263	.173	152	1.58	.339
816	207	.143	145	1.60	.342
871	101	.074	137	1.62	.345
983	49	.040	124	1.66	.351

TABLE II. - TEMPERATURE-DEPENDENT REPRESENTATION OF SHORT-TIME HASTELLOY X CREEP RESPONSE

Temperature, °C	Constants for creep equation* $\epsilon_{cr} = (\sigma/A)^n$ (t)	
	A	n
705	973	4.41
760	517	4.75
816	304	5.09
871	195	5.42
927	158	3.78
983	134	2.53

*Stress (σ) in MPa, creep strain rate (ϵ_{cr}) in percent, (t) in hours.

TABLE III. - RESULTS OF COMBUSTOR LINER SPECIMEN ANALYSES

(All results are for hoop direction at edge of louver lip)

	Elastic	Inelastic (6th cycle)
Max. strain, %	+.0135	-.100
Min. strain, %	-.361	-.448
Total strain range, %	.375	.348
Mean strain, %	-.174	-.274
Mean stress (MPa)	- 245	+ 138

ORIGINAL PAGE IS
OF POOR QUALITY

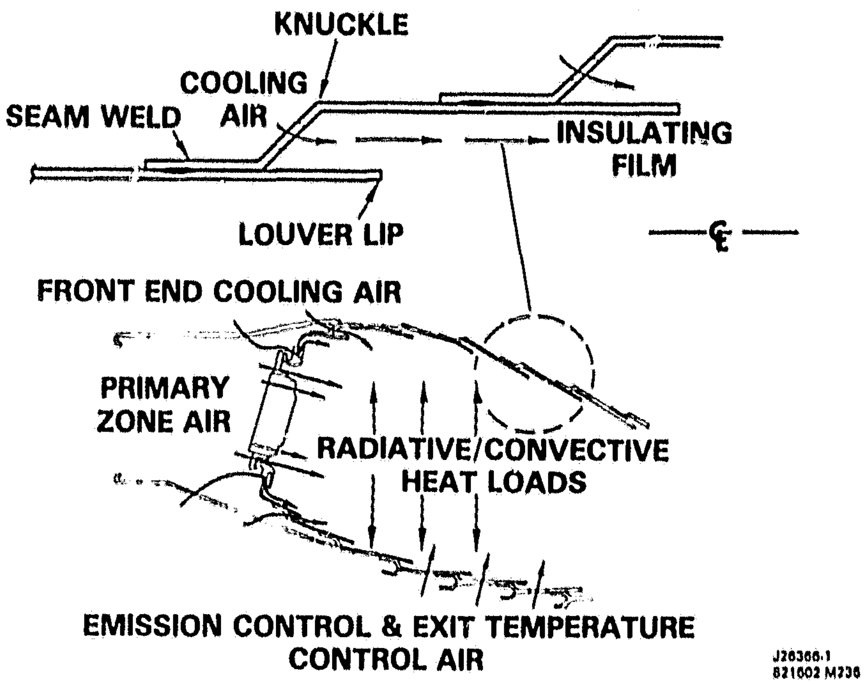

Figure 1. - Typical louver combustor liner construction and airflow distribution.

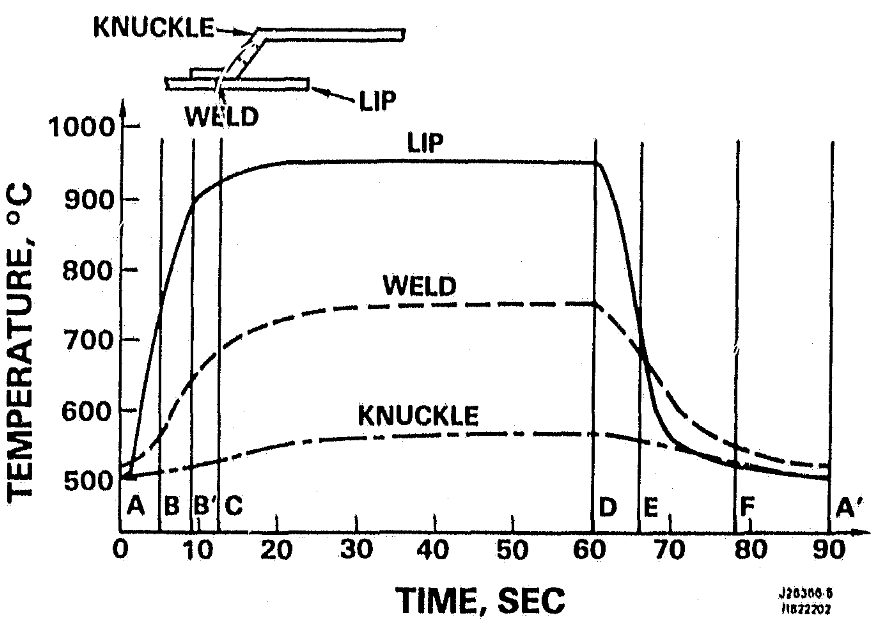

Figure 2. - Louver temperature response.

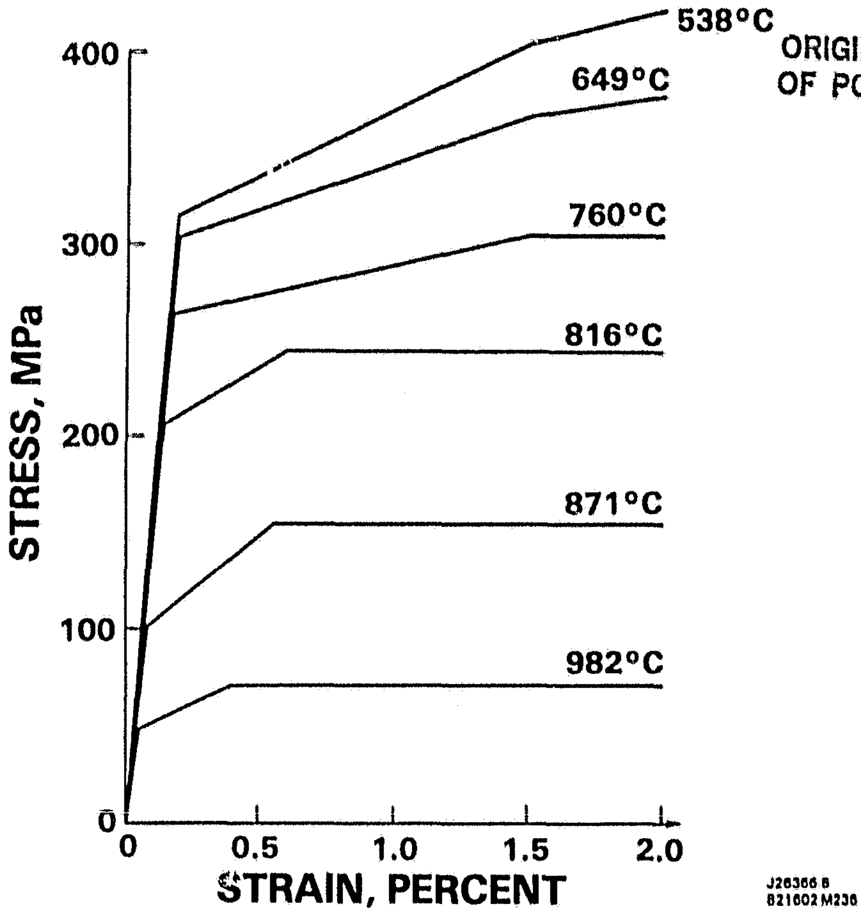

Figure 3. - Hastelloy X stress-strain representation (strain rate = 0.8%/min).

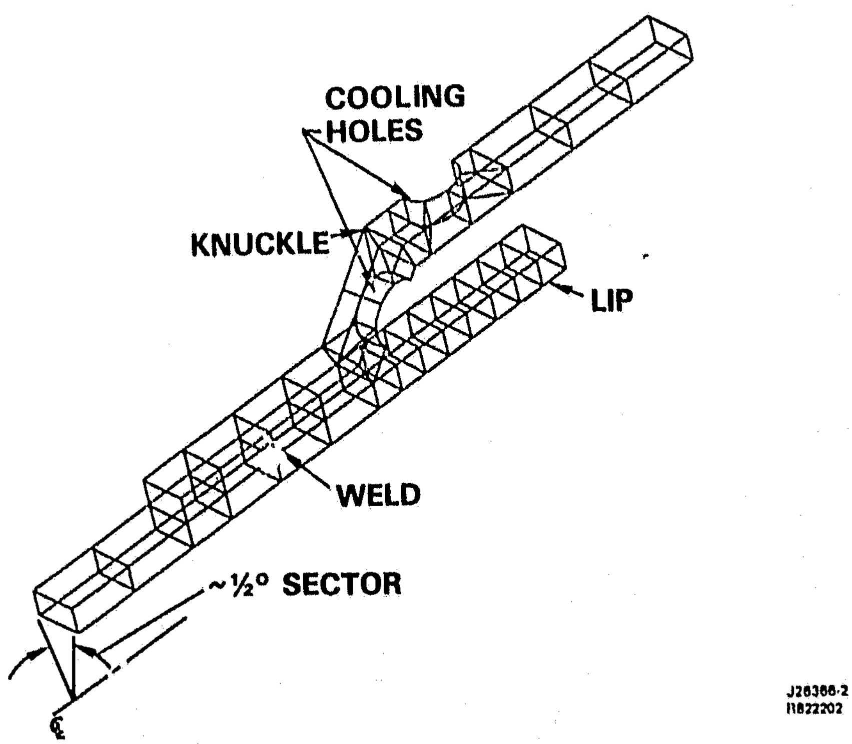

Figure 4. - Finite element model.

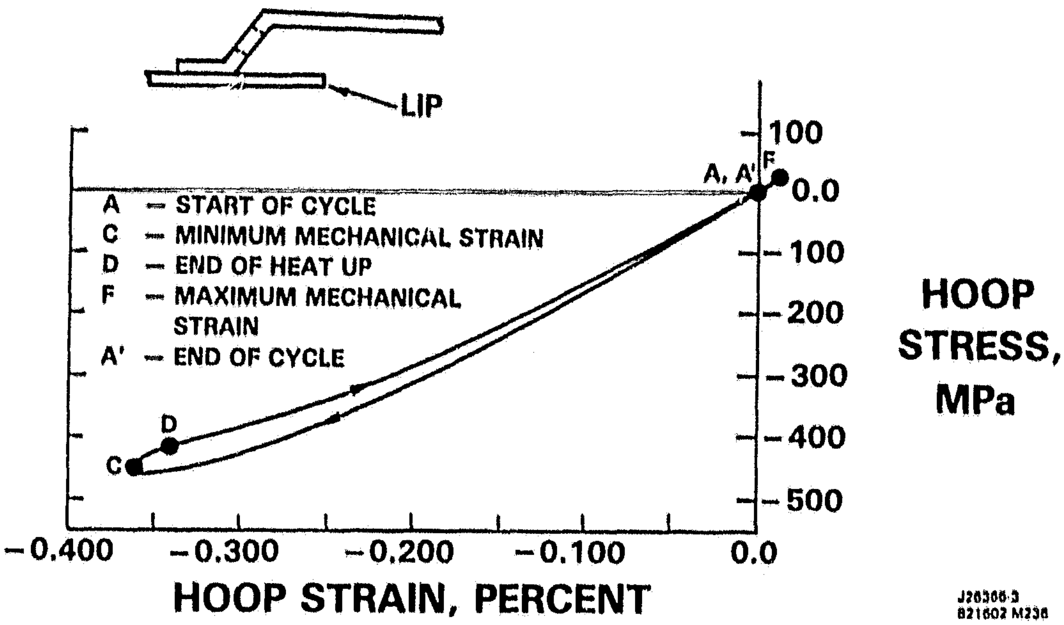

Figure 5. - Elastic analysis stress-strain response at louver lip.

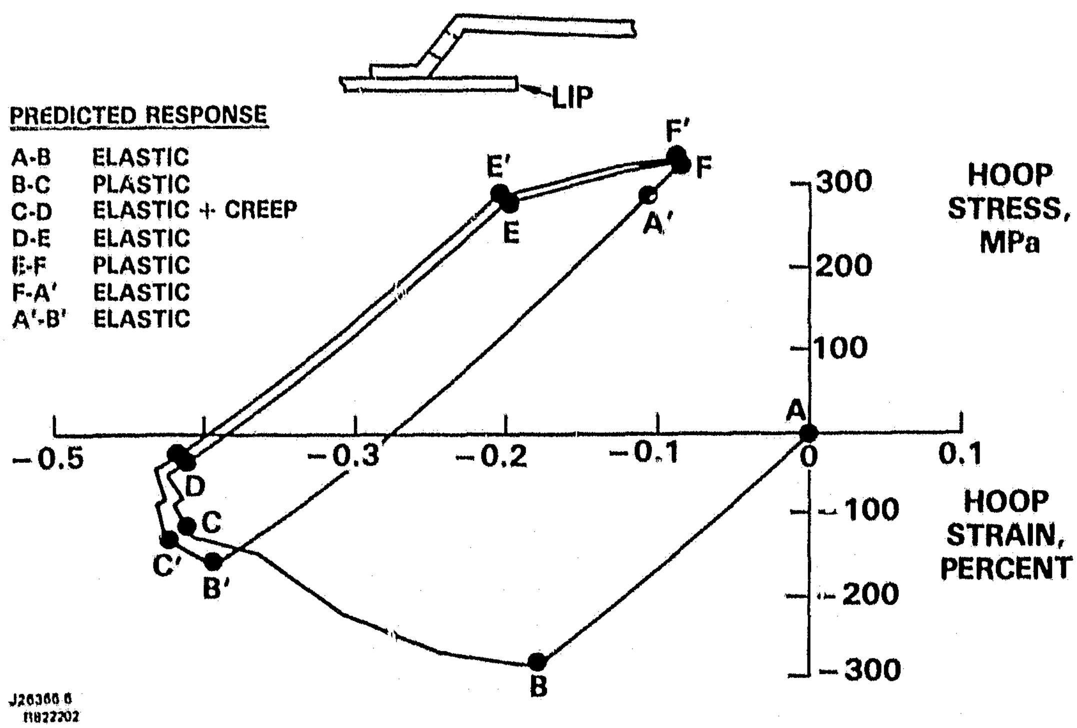

Figure 6. - Nonlinear analysis stress-strain response at louver lip.

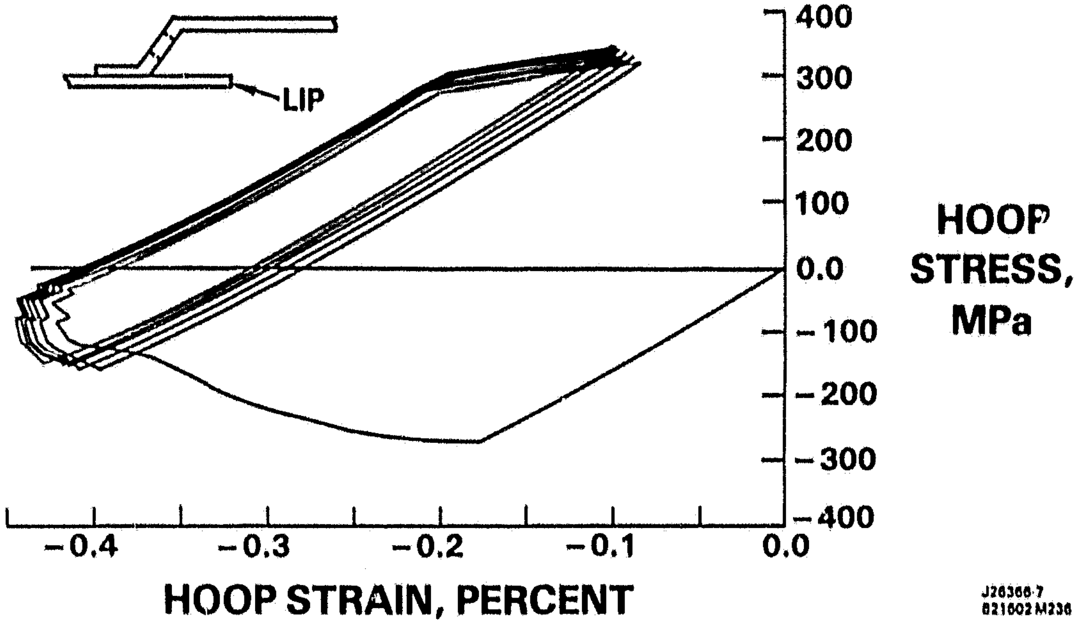

Figure 7. - Predicted louver lip response for six (6) loading cycles.

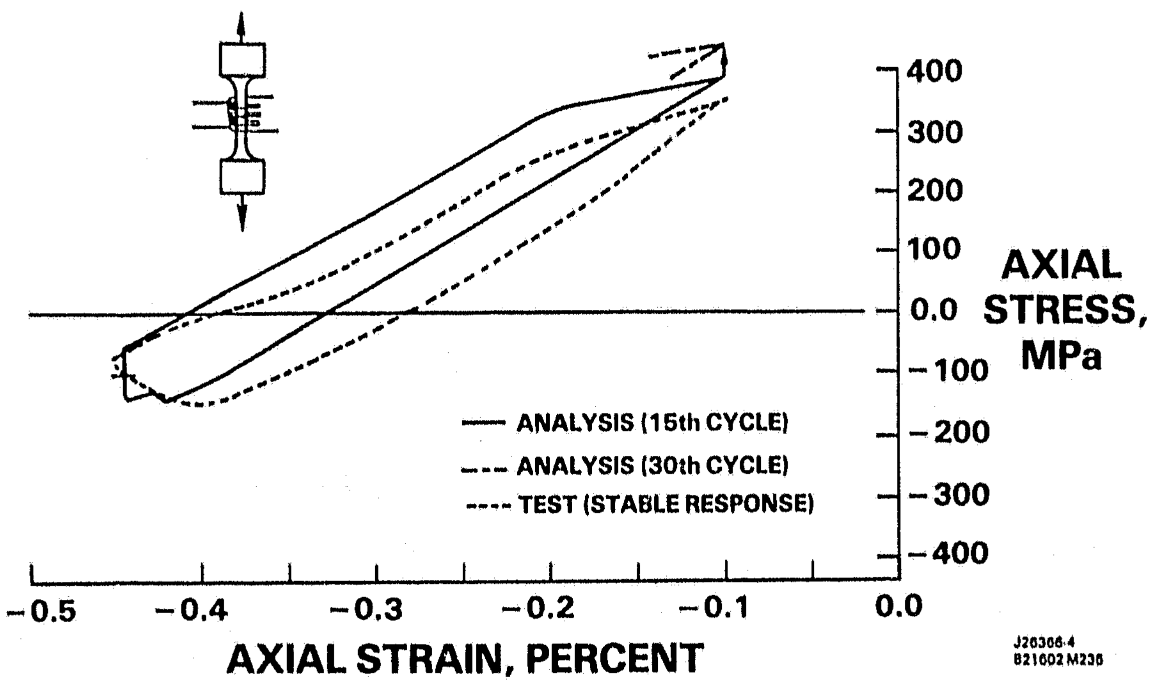

Figure 8. - Comparison of uniaxial thermo mechanical test and analytical results.